Size-Controlled Photochemical Synthesis of Niobium Nanoparticles

Dimitriy Malyshev,[a] Francisco Boscá,[b] Charles-Oneil L. Crites,[a] Geniece L. Hallett-Tapley,[a] José Carlos Netto-Ferreira,[c*] Emilio I. Alarcon,[a] and Juan C. Scaiano[a*]

[a] Department of Chemistry and Centre for Catalysis Research and Innovation, University of Ottawa, 10 Marie Curie, Ottawa K1N 6N5, Canada

[b] Instituto de Tecnologia Quimica (ITQ), Universidad Politecnica de Valencia, Av. de los Naranjos s/n, 46022, Valencia, Spain.

[c] Divisão de Metrologia Química, Instituto Nacional de Metrologia, Qualidade e Tecnologia-INMETRO, Duque de Caxias, 25250-020, Rio de Janeiro, Brazil.

Table of Contents

Experimental Procedures

General. Unless otherwise stated, all chemicals used for sample preparation were purchased from Sigma-Aldrich in the highest purity available and used as received. Irgacure 907 was a generous gift obtained from Ciba Specialty Chemicals (now BASF Global). HPLC grade CH_3CN was purchased from Sigma Aldrich and purified using a LC Technologist Solvent Purification System fitted with an alumina column. Bulk, commercial Nb_2O_5•H_2O was obtained from Companhia Brasileira de Metalurgia e Mineração (CBMM) in Brazil and used as received. All glassware was thoroughly cleaned, rinsed with nanopure water and dried at 130°C prior to use. Hot glassware was immediately sealed and purged with Industrial T (99.9%) argon gas after removal from the oven**.**

Preparation of acetylacetone stabilized Nb (V) (Nb(acac)$_5$) stock solution. A 208 mM stock solution of Nb(acac)$_5$ was prepared by simple ligand exchange with Nb (V) ethoxide in a amber vial. In a glove box under N_2 atmosphere, 2.0 mmol (0.5 mL) of niobium (V) ethoxide was added to 1.6 mL of CH_3CN followed by 10.7 mmol (1.1 mL) of acetylacetone and diluted to a final volume of 9.6 mL. The vial was sealed and allowed to stand for 20-30 minutes to allow for complete ligand exchange. The stock solution was stored under argon and at -10°C between uses.

Preparation of 500 mM Irgacure 907 (I-907) stock solution. A 500 mM stock solution was prepared by dissolving 1.40 g of I-907 in 10 mL of CH_3CN. The solution was stored in a 15 mL amber vial under argon at room temperature to prevent photodegradation. The presence of the acetylacetonate ligand was confirmed by Raman spectroscopy, where the presence of Raman shifts at 260 cm^{-1} (broad), 430 cm^{-1} and 880 cm^{-1} were indicative of ethanol release upon successful acac ligand exchange. (Figure S10)

Preparation of 4-(methylthio)benzaldehyde (MSBA) stock solution. A 0.5 M stock solution was prepared by dissolving 0.66 mL of MSBA into 10 mL CH_3CN. The mixture was stored under Ar gas at room temperature inside the sealed 15 mL amber vial.

Synthesis and stock solution preparation of isopropylmorpholine. *N*-isopropylmorpholine was synthesized and purified according to a previously reported method (Yamashiro, D., Li, C.H. *Int. J. Peptide Protein Res.* **1988**, *31*, 322-334). A 0.5 M stock solution of isopropylmorpholine in CH_3CN was then made for use in subsequent experiments.

NbNP Sample Preparation. 10.4 μM of $Nb(acac)_5$ (1.0 μL of 280 mM stock solution; 0.25 μmol) and varying concentrations of I-907 (using 500 mM stock solution; 60, 80, 100, 190, 260, 420, 520, 620, 730 μM) were added to 20 mL of CH_3CN in a 50 mL round bottom flask. The reaction mixture was shaken thoroughly, separated into the six 7 mm × 7 mm quartz cuvettes and irradiated for 5 hrs at 24 °C inside a Luzchem photoreactor equipped with 14 UVB blubs (λ=281-315 nm; 62 W/m^2). Samples were rotated to allow for homogeneous irradiation of the solutions.

Preparation of NbNP for XPS analysis. To obtain larger quantities of sample for XPS analysis, 150 μM $Nb(AcAc)_5$ and 10 mM I-907 precursors were added to a total volume of 100 mL. These particles were large in size (150-200 nm) to allow for ease of XPS analysis. The reaction was irradiated using UVB light for 10 hours in a quartz vessel. Following irradiation, the sample was transferred to 15 mL Falcon tubes and centrifuged at 8000 rpm for 30 minutes. The NbONP precipitate was resuspended in acetonitrile, centrifuged and washed once more with solvent. The wash was decanted off and the powder left to dry overnight in the fumehood.

Instrumentation. UV-visible spectra were carried out on a Cary 50 spectrophotometer. Samples were measured in the 7 mm × 7mm quartz cuvettes in which they were prepared (no sample dilution) and under argon or atmospheric conditions, as indicated. Fluorescence emission spectra were collected using a Photo Technology International spectrofluorometer equipped with a LPS-220 lamp power supply in a 1 cm × 1 cm quartz cuvette. The size of NbONP were determined using a JSM-7500F field emission scanning electron microscope (SEM) from JEOL Ltd. NbONP size was determined from an average of 150-200 particle measurements. The crystalline structure of the materials was assessed using high-resolution TEM (HRTEM). Both TEM and HRTEM were collected JEOL JEM-2100F field emission transmission electron microscope equipped with an ultra high-resolution pole-piece operating at 200kV. Elemental analysis of the NbONP was accessed using an Oxford Instruments X-ray energy dispersive spectrometer (EDS) attached to the JEM-2100F microscope. Solutions for SEM were prepared by dropping 10 mL of the reaction mixture onto a copper grid. For TEM analysis, samples were centrifuged (10000 rpm) and re-suspended in CH_3CN to ensure removal of any excess organic materials prior to deposition on the copper grid. X-ray photoelectron spectroscopy (XPS) was recorded using Kratos analytical model Axis Ultra DLD, using monochromatic aluminum Ka X-rays at a power of 140 watts. XPS samples were prepared by dropping 20 mL of sample onto a 1 cm × 1 cm silicon wafer and the solvent was evaporated prior to analysis. Gas chromatography-mass spectra (GC-MS) were recorded of non-diluted samples on an Agilent 6890N GC coupled with a 5973i mass selective detector. Raman spectra were collected using a single mode 785 nm laser (Innovative Photonic Solutions) with a maximum power output of 100 mW. The laser beam was passed through a band pass filter centred at 785 nm to filter out wavelength components in this wavelength region from the laser diode. A dichroic filter (R785RDC, Chroma Technologies Corp.) was use to reflect the light at an angle of 45° onto the sample and was further focused using a 40x microscopic objective lens. The Raman light was collected by a a fiber bundle (Fiberoptic System Inc., 26 multimode fiber) coupled to a Kaiser f/18i Spectrograph with a CCD camera. Andor SOLIS software was used for spectral data acquisition. Samples used for Raman spectroscopy were prepared as described using the aforementioned substrate concentrations in a 7 mm × 7 mm quartz laser cuvette under argon atmosphere. XPS spectra on fresh NbONP powders were recorded on a Kratos analytical model Axis Ultra DLD using monochromatic aluminium Ka X-rays at a power of 140 watts. XPS sputtering was achieved using Ar ion impact at 4 keV for 30 minutes using $\theta = 45°$. Measured sample currents were 1 μA over a 4 mm × 4 mm area using a flood gun calibrated for optimal peak shape and C-C carbon as the reference photoelectron for charge accumulation correction. XPS data was analyzed using CasaXPS software, Version 2.3.15 and all fittings obtained using a Gaussian/30% Laurentian and a Shirley baseline.

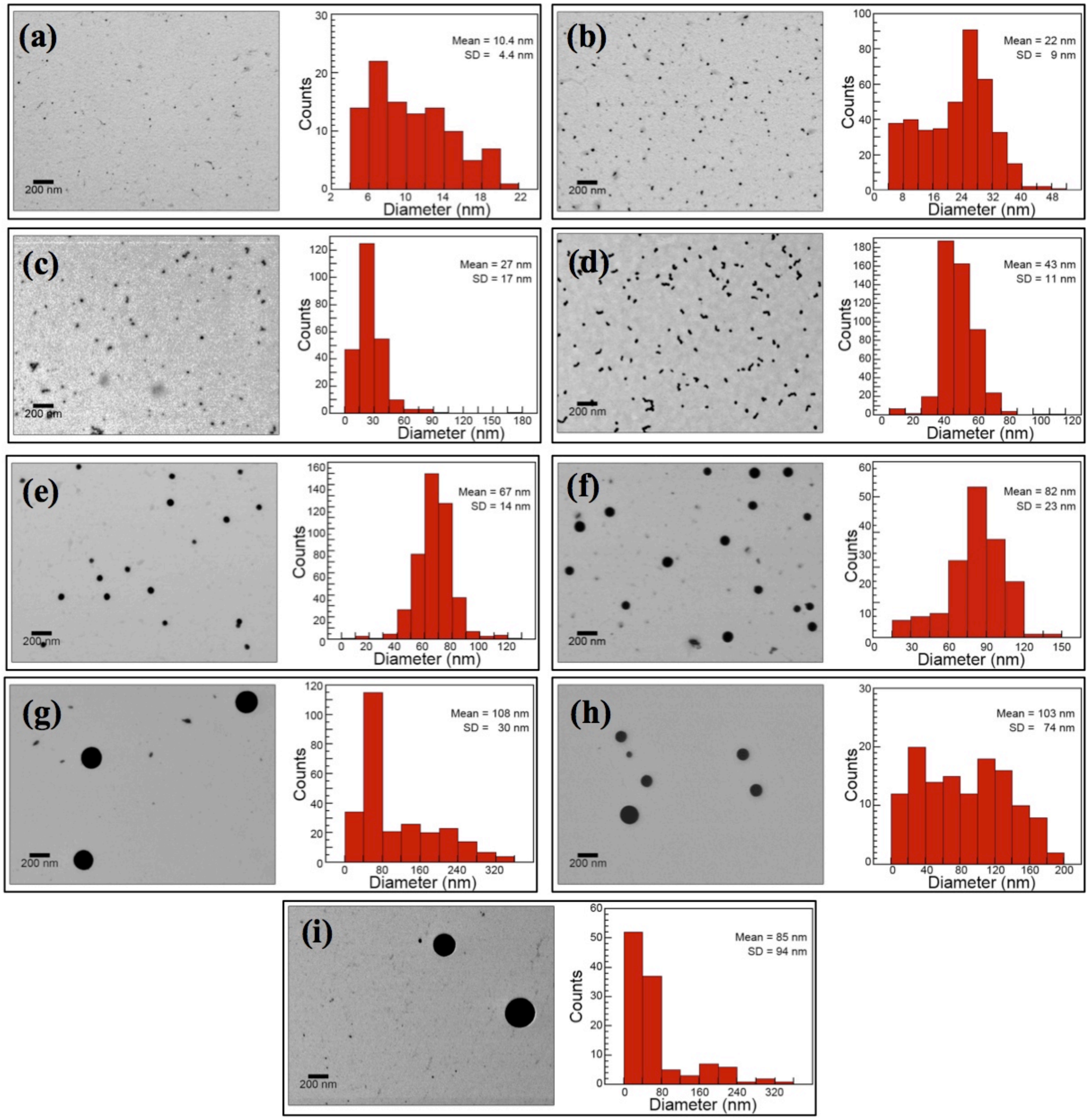

Figure S1. SEM analysis (left) and size distribution histograms (right) of NbONP prepared from 10 μM Nb(acac)$_5$ and **(a)** 60 μM, **(b)** 80 μM, **(c)** 100 μM, **(d)** 190 μM, **(e)** 260 μM, **(f)** 420 μM, **(g)** 520 μM, **(h)** 620 μM and **(i)** 730 μM I-907.

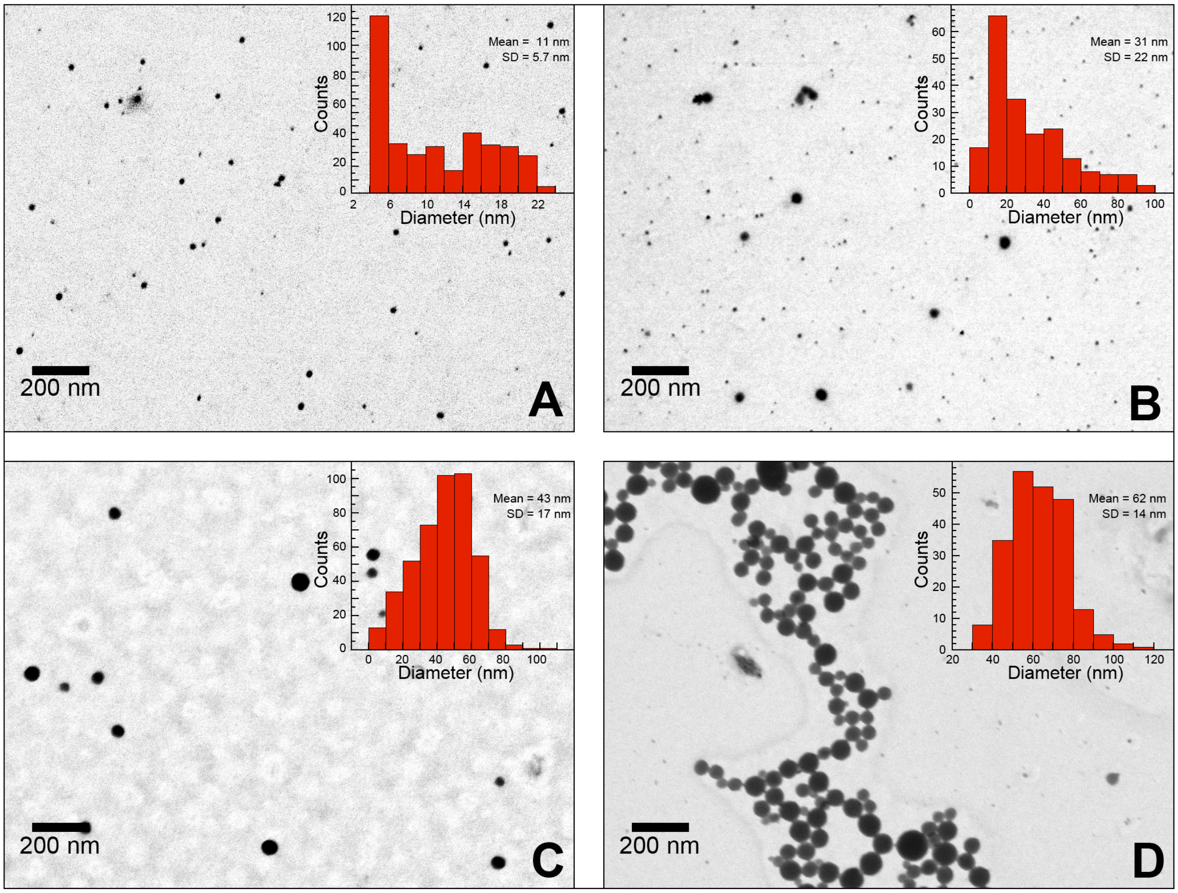

Figure S2. SEM images illustrating the formation of NbONP from 190 μM I-907 and 10 μM Nb(acac)$_5$ under argon atmosphere following **(A)** 10 min, **(B)** 30 min, **(C)** 60 min and **(D)** 300 min of UVB irradiation. Insets depict the corresponding nanoparticle size distribution histograms and suggest that the size of NbONP increases proportional to irradiation time and tends to terminate following 300 min of UVB excitation.

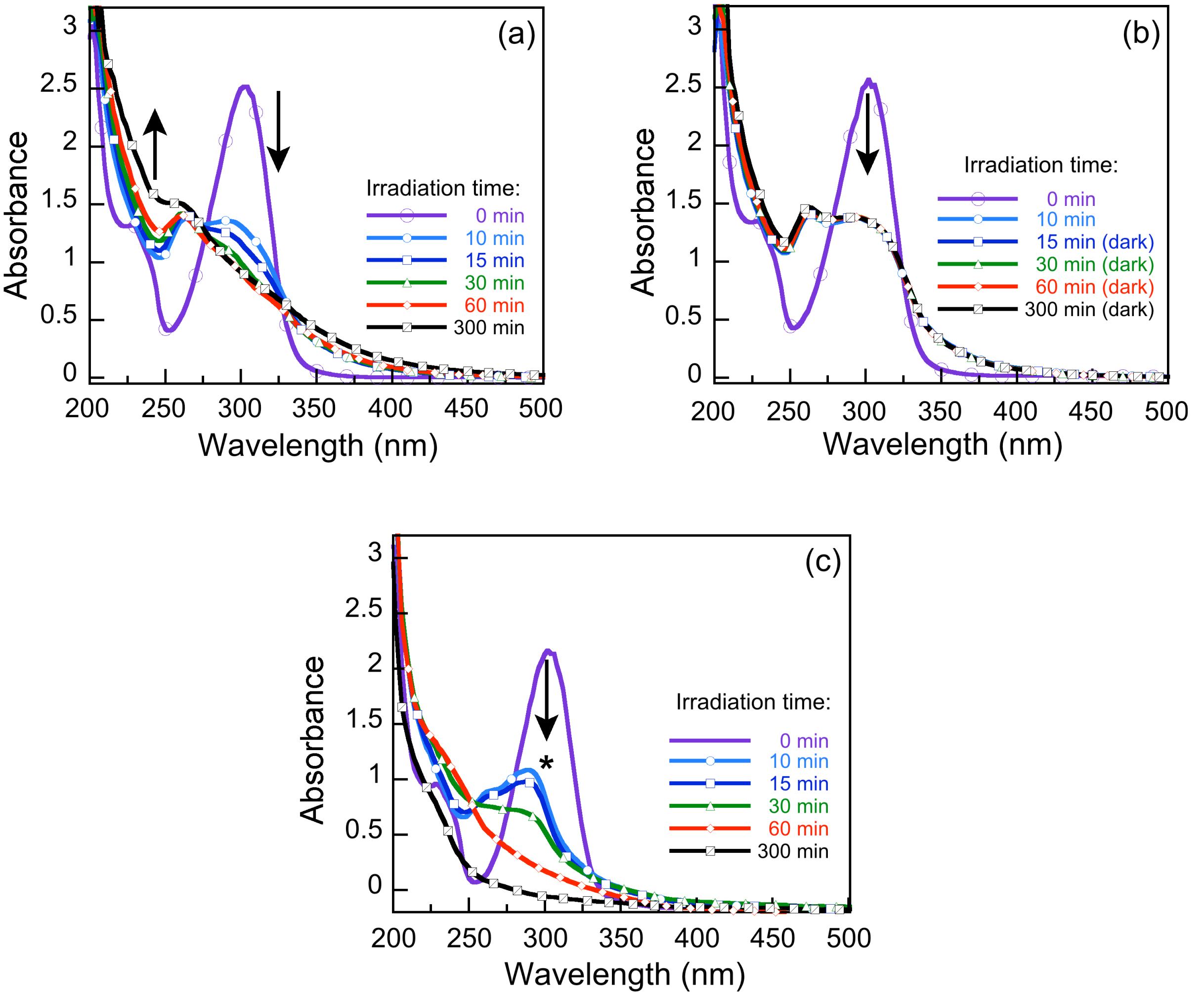

Figure S3. UVB irradiation of a CH_3CN solution of **(a)** 190 μM I-907 and 10 μM Nb(acac)$_5$ under argon, **(b)** 190 μM I-907 and 10 μM Nb(acac)$_5$ for 10 minutes, followed by storage of the sample under dark conditions (t = 15 min to t = 300 min) and **(c)** 190 μM I-907 under argon.

These plots clearly illustrate that UVB irradiation of the sample is required to promote complete NbNP growth, as is evidenced by the termination of NbNP formation (scattering observed at ~ 230 nm) and I-907 photodegradation (disappearance of absorbance at 310 nm) when the sample is removed from the excitation source and the sample placed in dark conditions. Disappearence of the 310 nm absorption band of I-907 is replaced by a broad peak at 290 nm, ascribed to the 4-(methythio)benzaldehyde (MSBA) (*) following irradiation of the photoiniator itself and comparision to a UV-visible absorption spectrum of an authentic sample.

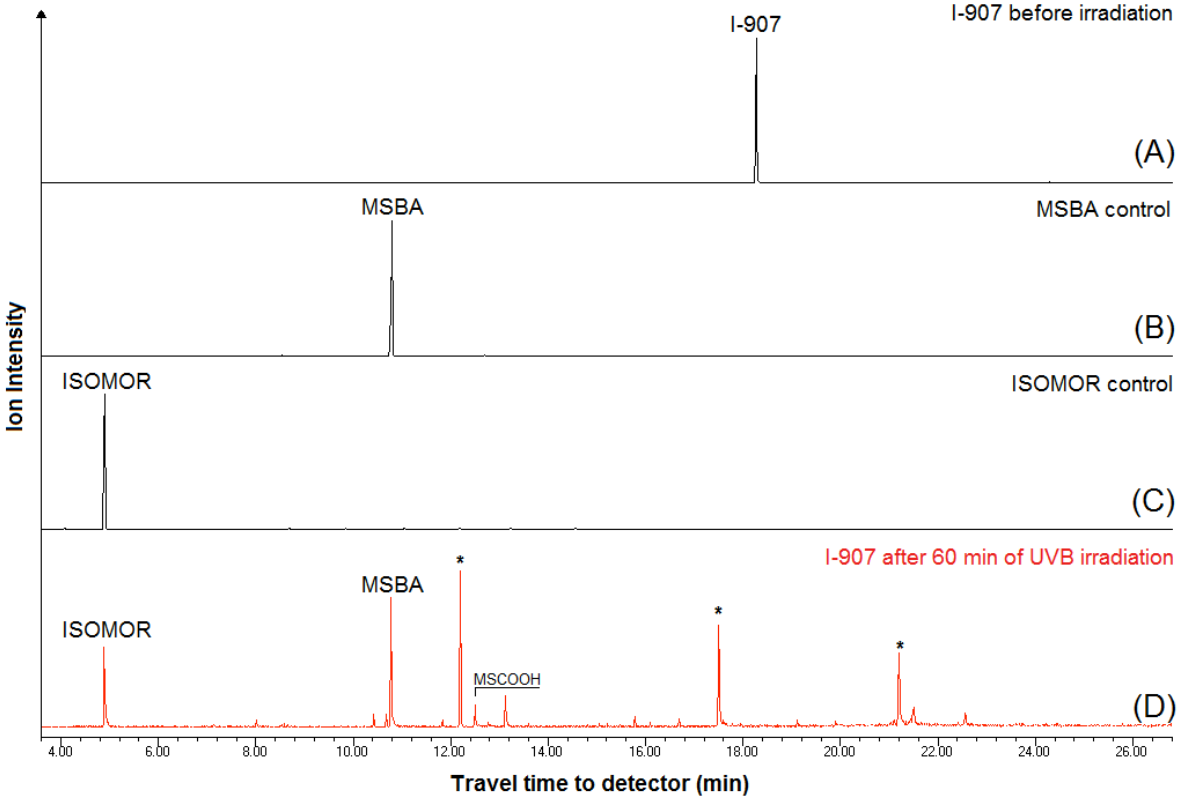

Figure S4. GC analysis of (A) 190 μM I-907, (B) 190 μM MSBA, (C) 190 μM isopropylmorpholine and (D) a solution of 190 mM I-907 after 60 minutes of UVB irradiation (all in CH_3CN). Results confirm the formation of the two major photoproducts: MSBA and
5 isopropylmorpholine. Note: * denote the formation of secondary photoproducts.

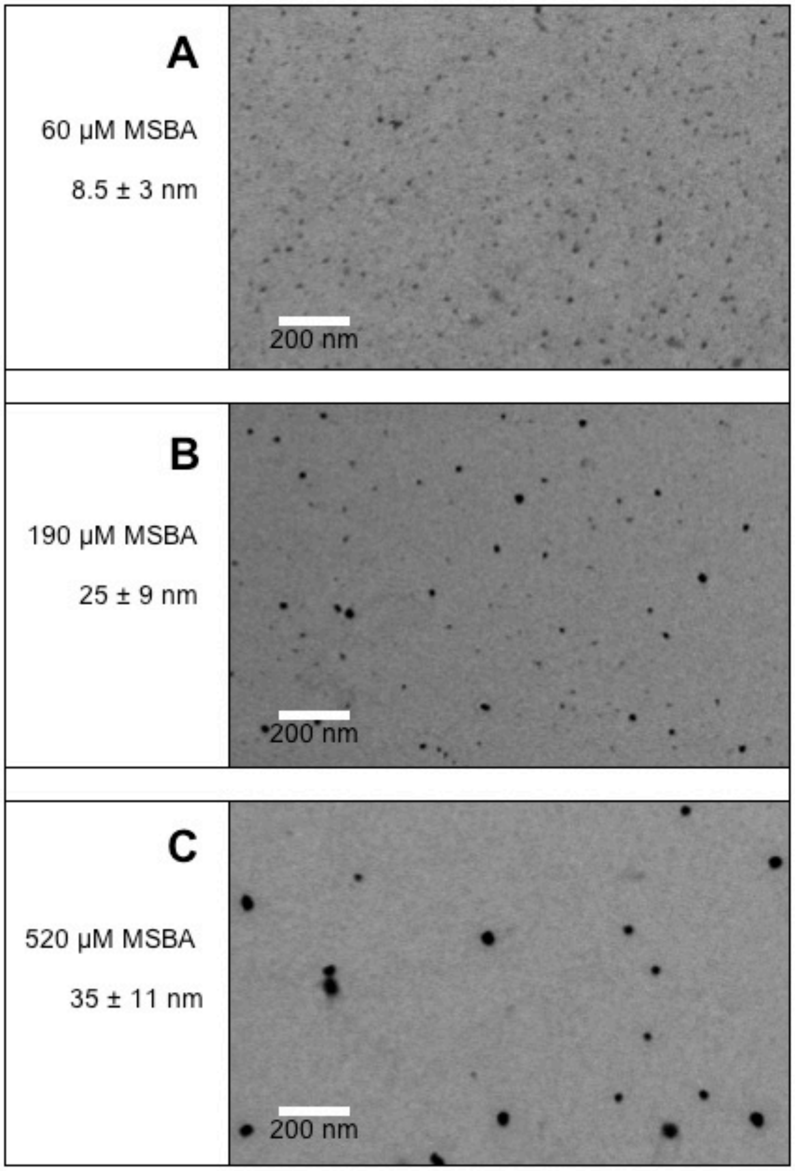

Figure S5. Representative SEM images of 10 µM Nb(acac)$_5$ and **(A)** 60 mM, **(B)** 190 mM and **(C)** 520 µM MSBA. From the average sizes presented to the left of each image, the diameter of NbONP was found to increase with [MSBA].

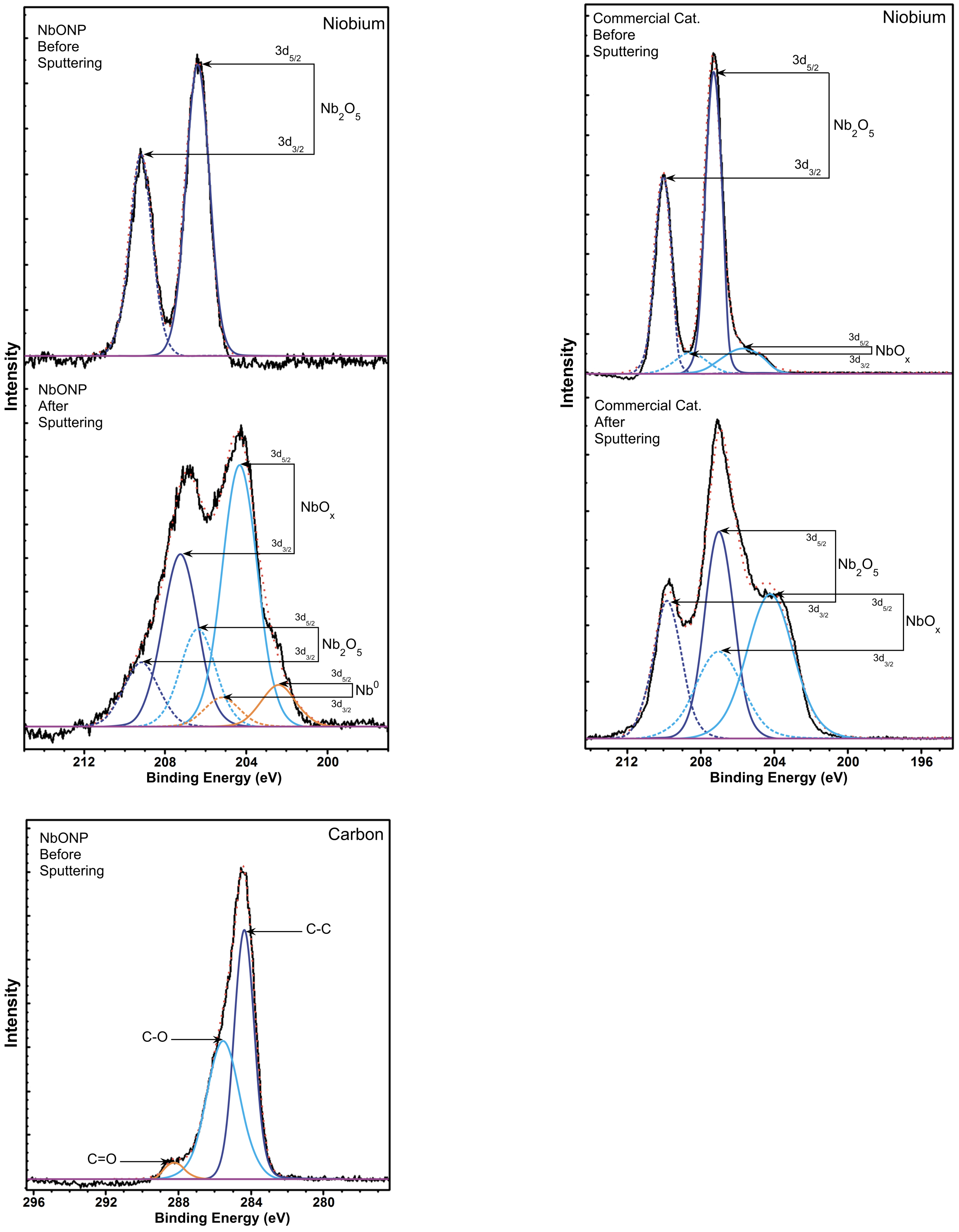

Figure S6. XPS analysis of the niobium region before and after ionic sputtering and 1s C region of NbONP (left) prepared using 10 mM I-907 and 150 µM Nb(acac)$_5$ in CH_3CN under argon. XPS analysis of the niobium region before and after ionic sputtering of a commercial Nb_2O_5 sample obtained from CBMM, Brazil.

XPS analysis of NbONP indicated an absence of the Nb^0 oxidation state within the nanomaterial, suggesting that all of the particles undergo complete oxidation. Before sputtering, Nb^{5+} was detected from binding energies at 206.4 and 209.2 eV, respectively.[S1, S2] After sputtering, Nb metal, remaining Nb^{5+} and other lower Nb oxide (NbO_x) states were observed. From comparison with ionic sputtering of an authentic $Nb_2O_5 \bullet H_2O$ samples (CBMM, Brazil), it is evident that the formation of Nb^0 identified in the XPS spectrum of NbONP after sputtering is not due effects of ion bombardment during the sputtering process.

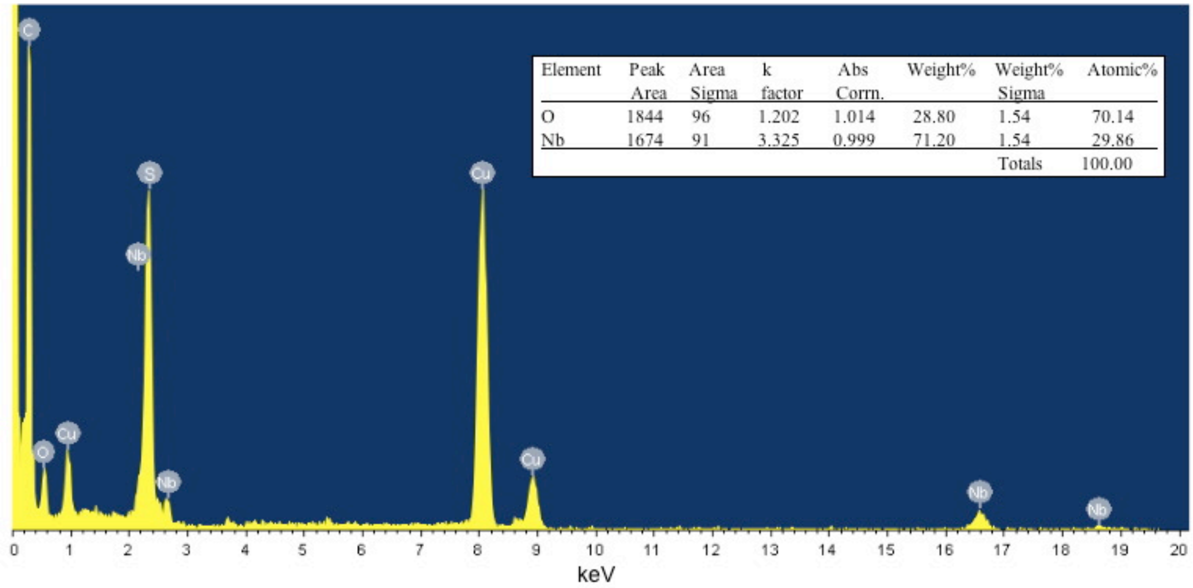

Element	Peak Area	Area Sigma	k factor	Abs Corrn.	Weight%	Weight% Sigma	Atomic%
O	1844	96	1.202	1.014	28.80	1.54	70.14
Nb	1674	91	3.325	0.999	71.20	1.54	29.86
						Totals	100.00

Figure S7. EDS analysis NbONP prepared from 520 µM I-907 and 10 µM Nb(acac)$_5$ followed by deposition onto a copper grid. The ratio of atomic % for O and Nb, (~5/2) supports the presence of Nb_2O_5 on the nanoparticle surface.

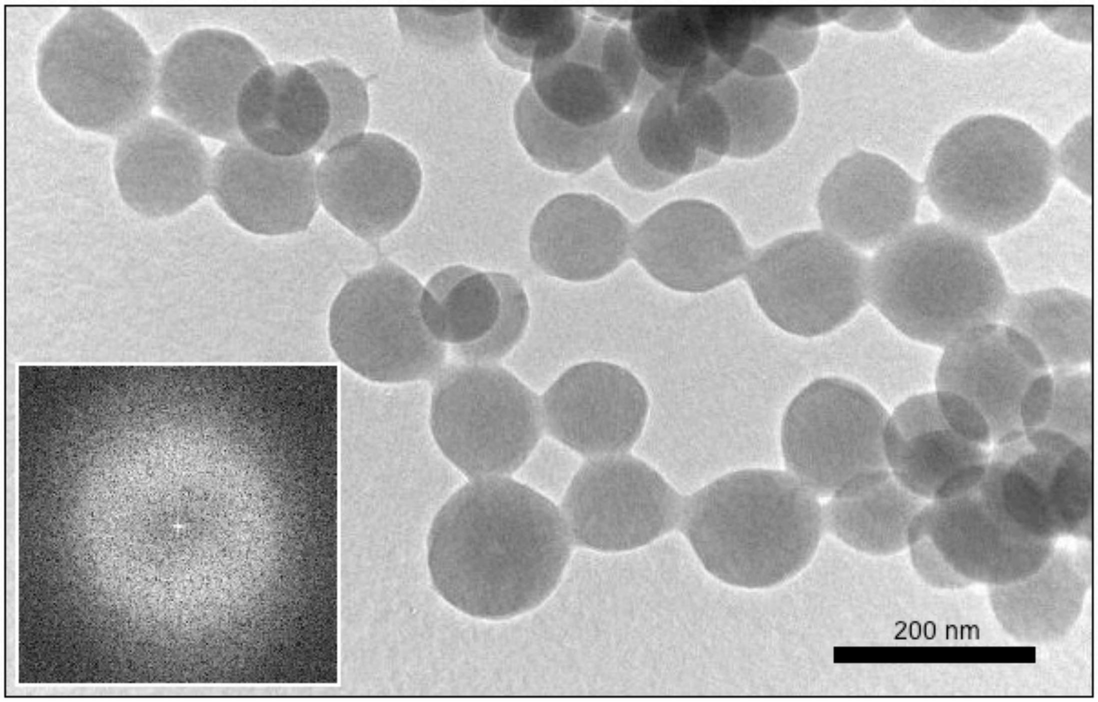

Figure S8. TEM analysis of NbONP prepared from a solution of 520 µM I-907 and 10 µM Nb(acac)$_5$. Inset depicts HRTEM diffraction pattering illustrating the absence of a crystal lattice and the amphorous nature of these nanostructures.

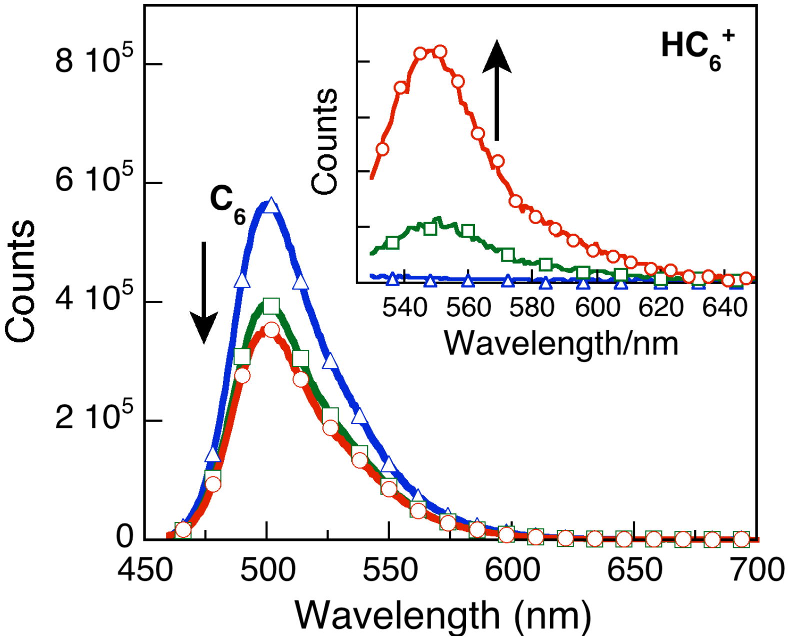

Figure S9. Fluoresence emission spectrum of a 0.9 μM coumarin-6 (C_6) control (Δ), 0.9 μM C_6 in the presence of 91 fM (□) and 0.4 pM (○) NbONP. NbONP were prepared using 260 μM I-907 and 10 μM Nb(acac)_5. Addition of NbONP results in an immediate decrease in the intensity of C_6 emission (λ_{emit} = 500 nm, λ_{ex} = 450 nm). Inset presents an increase in emission at λ_{emit} = 555 nm (λ_{ex} = 520 nm) ascribed to the protonated form of the C_6 dye (HC_6^+).

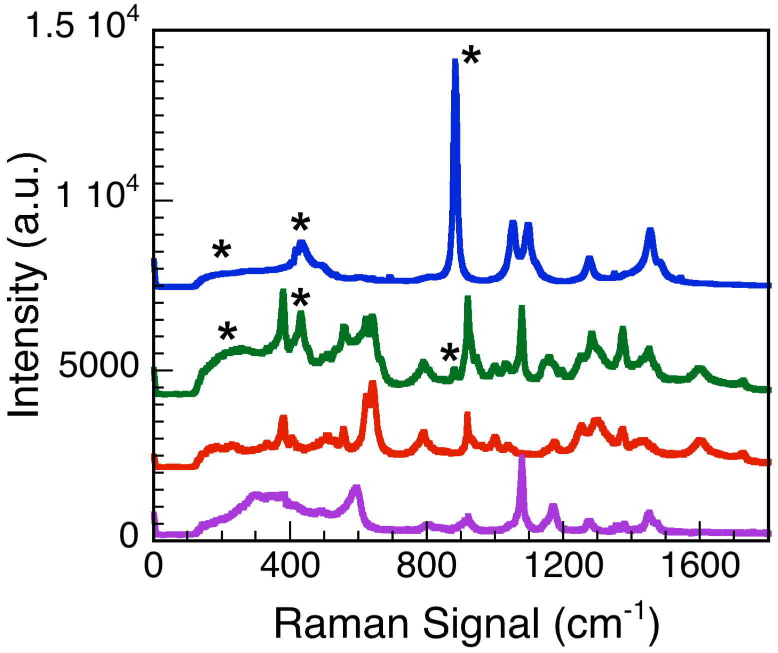

Figure S10. Raman spectra of ethanol (—), Nb(acac)$_5$ (—), acetylacetone (—) and Nb(OCH$_2$CH$_3$)$_5$ (—).

Peaks denoted by * label the similarities between ethanol and Nb(acac)$_5$ generated from Nb(OEt)$_5$ and acetylacetone and indicate ethanol release in the solution due to successful acac ligand exchange.

Table S1. XPS binding energies obtained following peak fitting of NbONP before and after sputtering.

a) NbONP; Nb analysis (before sputtering)

Peak Identity	Peak Type	BE (eV)	FWHM	R.S.F	Fit	Area	% Area
Nb_2O_5	$3d_{5/2}$	206.4	1.32	8.21	GL(30)	1865	59.5
	$3d_{3/2}$	209.2	1.32	8.21	GL(30)	1270	40.5

5 b) NbONP; Nb analysis (after sputtering)

Peak Identity	Peak Type	BE (eV)	FWHM	R.S.F	Fit	Area	% Area
Nb_2O_5	$3d_{5/2}$	206.4	2.23	8.21	GL(30)	1284	14.7
	$3d_{3/2}$	209.2	2.23	8.21	GL(30)	847	9.8
NbO_x	$3d_{5/2}$	204.4	2.23	8.21	GL(30)	3432	39.2
	$3d_{3/2}$	207.3	2.23	8.21	GL(30)	2265	25.9
Nb^0	$3d_{5/2}$	202.4	2.23	8.21	GL(30)	546	3.2
	$3d_{3/2}$	205.2	2.23	8.21	GL(30)	387	4.4

c) NbONP; 1s C analysis (before sputtering)

Peak Identity	Peak Type	BE (eV)	FWHM	R.S.F	Fit	Area	% Area
C-C	1s	284.4	1.29	1.00	GL(30)	7976	50.3
C-O	1s	285.5	2.16	1.00	GL(30)	7360	46.4
C=O	1s	288.3	1.27	1.00	GL(30)	523	3.3

d) Bulk, commercial Nb_2O_5•H_2O; Nb analysis (before sputtering)

Peak Identity	Peak Type	BE (eV)	FWHM	R.S.F	Fit	Area	% Area
Nb_2O_5	$3d_{5/2}$	206.7	1.02	8.21	GL(30)	16465	49.1
	$3d_{3/2}$	209.5	1.02	8.21	GL(30)	10867	32.4
NbO_x	$3d_{5/2}$	205.2	2.21	8.21	GL(30)	3744	11.2
	$3d_{3/2}$	208.0	2.21	8.21	GL(30)	2471	7.4

10

e) Bulk, commercial Nb_2O_5•H_2O; Nb analysis (after sputtering)

Peak Identity	Peak Type	BE (eV)	FWHM	R.S.F	Fit	Area	% Area
Nb_2O_5	$3d_{5/2}$	207.0	1.83	8.21	GL(30)	14459	28.9
	$3d_{3/2}$	209.8	1.83	8.21	GL(30)	9543	19.1
NbO_x	$3d_{5/2}$	204.2	2.96	8.21	GL(30)	16238	32.5
	$3d_{3/2}$	207.0	2.96	8.21	GL(30)	9791	19.6

References

S1. Ma, Q.; Rosenbert, R.A. *Appl. Surf. Sci.* **2003**, *206*, 209-217.
S2. Mukherjee, M.; Basu, S., Ghosh, B., Chakravorty, D. *Appl. Surf. Sci.* **2007**, *253*, 8463-8469.